

# Structure of Guar in Solutions of H<sub>2</sub>O and D<sub>2</sub>O: An Ultra-Small-Angle Light-Scattering Study

M. R. Gittings,<sup>1a</sup> Luca Cipelletti,<sup>\*,1b,c</sup> V. Trappe,<sup>1b,d</sup> D. A. Weitz,<sup>1b,e</sup> M. In,<sup>1a</sup> and C. Marques<sup>1a</sup>

Complex Fluids/CNRS Laboratory, Rhodia Inc., CN 7500, Cranbury, New Jersey 08512-7500, and Department of Physics, University of Pennsylvania, 209 South 33rd Street, Philadelphia, Pennsylvania 19104-6396

Received: December 13, 1999; In Final Form: February 11, 2000

We examine the structure of guar as a function of concentration in both H<sub>2</sub>O and D<sub>2</sub>O using several different scattering techniques. The range of scattering vectors spans 5 decades ( $143 \text{ cm}^{-1} < q < 10.3 \times 10^6 \text{ cm}^{-1}$ ), providing insight into the supramolecular and local organization of the chains. This allows us to directly characterize the large-scale aggregate structure of the guar, which can be on the order of  $100 \mu\text{m}$ . The aggregates are most likely loosely interconnected with single chains and other aggregates, and the structure and organization are critical in determining solution viscoelastic properties. The solubility is poorer in D<sub>2</sub>O, as evidenced by larger aggregates, higher scattering intensities, a slightly higher fractal dimension, and a sublinear concentration dependence of the intensity. Aggregates were found in dilute neutral guar solutions as well as in cationic guar solutions (in H<sub>2</sub>O), whether screened or unscreened. The presence of aggregates at all concentrations for neutral and charged guar indicates the difficulty in determining a molecular weight of the guar molecule.

## Introduction

Guar is a naturally occurring (neutral) polysaccharide extracted from the guar gum bean plant and is widely used in industrial applications including food,<sup>2</sup> oil recovery,<sup>3</sup> and personal care<sup>4,5</sup> to control viscoelastic properties. Only a small amount of guar is needed to dramatically increase the viscosity. These viscoelastic properties are a direct consequence of the structures that are formed by the gum and their dependence on concentration. While rheological studies on guar abound,<sup>6–8</sup> little is known about the actual structure and organization of the molecules in solution. Guar consists of a mannose backbone with random substitutions of galactose in a ratio of 1.6:1 (Figure 1). Because of the random nature of the substitution, galactose-rich and galactose-poor regions are formed. The less soluble galactose-poor regions can associate to form partially crystalline complexes, resulting in structures which can vary in size over a large range of length scales; it is these structures which have the most important consequences for viscoelastic properties.<sup>8–11</sup> Thus, a wide range of accessible scattering vectors is essential to fully characterize the structure of guar.

In this paper we report the results of scattering studies on neutral guar as a function of concentration in solutions of both H<sub>2</sub>O and D<sub>2</sub>O. The use of D<sub>2</sub>O solutions was necessary to obtain proper contrast match conditions for neutron scattering data at a high scattering vector; however, these solutions were also studied at lower scattering vectors with light scattering to compare solubility properties with those of H<sub>2</sub>O solutions. We attain the requisite range of scattering vectors by combining light scattering at both intermediate angles and ultralow angles. Over a wide range of scattering vectors, we observe a power-law dependence of the intensity on scattering vector, indicating the presence of fractal structures. Fractal scaling extends to extremely small angles, revealing the presence of very large structures with length scales as large as  $100 \mu\text{m}$ . All the data are consistent with diminished solubility in D<sub>2</sub>O. Additionally, a cationic form of the guar molecule was tested which also showed the presence of aggregates indicating that the aggrega-

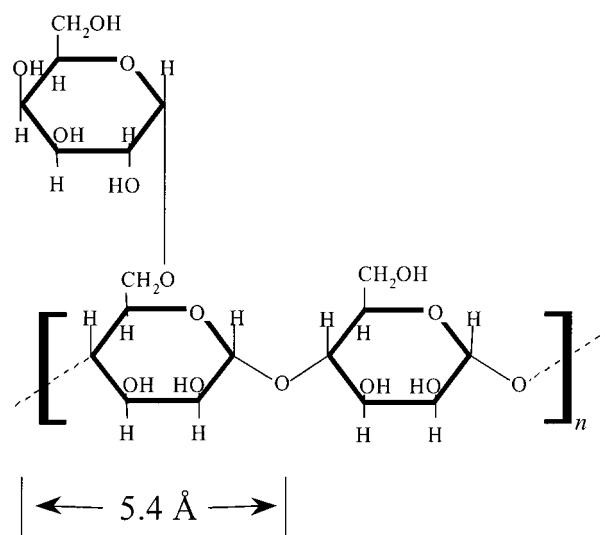


Figure 1. The guar molecule.

tion is intrinsic to guar and does not depend on Coulomb interactions of any sort. The presence of these large structures highlights the difficulty in using light scattering to determine the molecular weight of guar.

## Theoretical Background

Scattering techniques provide information on the conformation and organization of macromolecules in solution. The scattering intensity  $I$  is measured as a function of the magnitude  $q$  of the scattering vector, defined by

$$q = (4\pi n/\lambda) \sin(\theta/2) \quad (1)$$

Here  $n$  is the refractive index of the solvent,  $\lambda$  is the in vacuo wavelength of the source, and  $\theta$  is the scattering angle. Static light scattering probes the structure of the solution on length scales of order  $q^{-1}$ . Hence, the low- $q$  regime ( $q < R^{-1}$ , where

$R$  is the size of the macromolecule) provides information on the *supramolecular* structure of the system, that is, on the spatial organization of the system on length scales larger than the size of the molecule. On the contrary, in the high- $q$  limit,  $q \gg R^{-1}$ , scattering probes length scales on the order of a few monomer lengths or less. The intermediate scattering vector regime provides insight into the conformation of individual polymer chains within the macromolecules.

The morphology of macromolecules in solution is usually described in terms of the fractal dimension  $d_f$ , defined by the scaling law  $M \propto l^{d_f}$  where  $M$  is the mass enclosed in a "blob" of size  $l$ .<sup>12</sup> For an object with fractal dimension  $d_f$ , the scattered intensity decreases with  $q$  according to the power law<sup>12</sup>

$$I(q) \propto q^{-d_f} \quad (2)$$

Thus, static scattering allows a direct measure of the fractal dimension. For sufficiently large  $q$ , the fractal dimension reflects the local rigidity in the molecular chain,  $d_f$  being unity for length scales smaller than the persistence length. Note that neutron or X-ray scattering may be needed to probe such small length scales. At intermediate scattering vectors, the value of the fractal dimension reflects the relative solubility of the chain. For unbranched chains, the pivotal point is  $d_f = 2$ , which indicates a Gaussian (or random walk) conformation in  $\theta$  solvent conditions. For  $d_f \leq 2$ , the chain is more extended and is considered to be in good solvent conditions, whereas, for  $d_f > 2$ , the chain is in a more collapsed state and in poorer solvent conditions. The presence of branching will also typically lead to an increase in fractal dimension. At smaller  $q$ , the intensity scattered by dilute solutions typically deviates from the fractal regime described by eq 2 and exhibits a roll-off to a plateau. In dilute solutions, the position of the roll-off reflects the size  $R$  of the solute molecule. By contrast, the persistence of the fractal regime at very small scattering vectors ( $q \ll R^{-1}$ ) reveals the existence of structures on length scales larger than  $R$ ; this can result from the presence of large aggregates or from entanglements in concentrated solutions. In these cases, the fractal dimension at low  $q$  provides a measure of the supramolecular organization of the solution. A roll-off may be visible at even lower  $q$ , indicating the correlation length (in a network of entangled polymers), or the size of aggregates in solution.

### Experimental Method

**Materials.** Unmodified guar galactomannan (LJX-2) was obtained from Rhodia Inc. and purified by first dissolving in Millipore (0.22  $\mu\text{m}$  filtered, deionized, distilled) water, centrifuging to remove insoluble matter, precipitating with isopropyl alcohol, and, finally, drying under vacuum. The resulting white fibers were then ground to a fine consistency with a coffee grinder and stored in a desiccator. The moisture content was 8.7%. The intrinsic viscosity  $[\eta]$  in  $\text{H}_2\text{O}$  was found to be 21 dL/g, which gives a predicted overlap concentration  $c^*$  of 0.19 g/dL (using  $c^* \approx 4/[\eta]$ ). The intrinsic viscosity in  $\text{D}_2\text{O}$  was not measured.

The cationic guar was also obtained from Rhodia and purified. This guar is a modified form of the neutral guar with 14% of the hydroxyl groups randomly replaced by quaternary propylammonium groups which remain fully ionized in aqueous solution without pH adjustment. The intrinsic viscosity of the cationic guar depends on the salt concentration, ranging from 454 dL/g without added salt to 16.2 dL/g in 0.5 M NaCl (at room temperature) in  $\text{H}_2\text{O}$ -based systems. Such variations in the intrinsic viscosity are typical for polyelectrolytes.<sup>13</sup> Using

$c^* \approx 4/[\eta]$ , we estimate an upper bound for the overlap concentration of 0.25 g/dL.

Solutions were made by adding the dry guar powder to water ( $\text{H}_2\text{O}$  or  $\text{D}_2\text{O}$ ) in clean glass scintillation vials. The  $\text{D}_2\text{O}$  was obtained from Cambridge Isotope Laboratories and was 99.9% pure. Reversing the order of addition made dissolution of the guar more difficult. Immediately after addition, the solutions were shaken briskly by hand to disperse the guar. They were then rotated on a spinning wheel for at least 1 day at the highest possible speed that allowed mixing to occur. Previous work in our laboratory showed that guar solutions prepared using a magnetic stirrer had larger and more numerous aggregates; thus, this method was avoided. All solutions were stored at 6  $^\circ\text{C}$  to prevent degradation. No changes in the solution structure were observed upon refrigeration. Although the solvents were filtered with 0.22  $\mu\text{m}$  hydrophilically modified Teflon Millipore filters, the guar solutions were not filtered in order not to disturb the molecular structure and makeup of the solution.

**Scattering Methods.** The ultra-small-angle light-scattering apparatus (USALS) is described in detail elsewhere,<sup>14</sup> and only a brief account will be given here. A collimated laser beam impinges onto the sample, which is contained in a flat cell. Both the transmitted and the scattered light are collected by a lens (L1) in whose focal plane a beam stop blocks the transmitted beam. We use an objective lens to image the focal plane of L1 onto the sensor of a charge-coupled-device camera (CCD). To obtain the scattered intensity  $I(q)$ , the CCD output is averaged over rings of pixels centered about the optical axis of the apparatus, which correspond to the same magnitude  $q$  of the scattering vector. Care is taken to correct the data for the contribution of the CCD dark noise and for that of the stray light. The setup allows us to measure  $I(q)$  over almost 2 decades of scattering vectors, in the range  $150 \text{ cm}^{-1} < q < 12\,000 \text{ cm}^{-1}$ , corresponding to angles from  $0.06^\circ$  to  $4^\circ$ .

Static light scattering at higher scattering vectors (SLS,  $30\,000 \text{ cm}^{-1} < q < 307\,000 \text{ cm}^{-1}$ ) was performed using a Brookhaven Instruments Corp. (BIC) light-scattering apparatus with a 200SM goniometer, a 9000AT digital correlator, and a Lixel argon ion laser (model 95, 514.5 nm wavelength). Software from BIC (SLSW program) was used to automate the measurement and process the data. In this setup, a photomultiplier tube collects the scattered light intensity at each designated scattering angle. Only the lowest measured intensity values were accepted via a dust cutoff routine that is specified within the SLSW program (dust cutoff 10, 10–30 repetitions). Measurements were taken at a laser power between 4 and 8 mW and at a temperature of 25  $^\circ\text{C}$ .

To show the behavior of guar solutions at very small length scales, we include a set of small-angle neutron scattering (SANS) data for a  $\text{D}_2\text{O}$  solution. The data were collected on the time-of-flight small-angle diffractometer at the Intense Pulsed Neutron Source at Argonne National Laboratory. A detailed discussion on the SANS data for guar in  $\text{D}_2\text{O}$  is presented elsewhere.<sup>15</sup>

### Results and Discussion

The scattering profile for a 0.46% (w/w) guar solution in  $\text{D}_2\text{O}$  is examined first since the data span the widest scattering vector range. The data are shown in Figure 2, where the scattering intensity is plotted against  $q$  on a double logarithmic scale. The data for this particular sample were collected using USALS, SLS, and SANS instrumentation at low, intermediate, and high scattering vectors, respectively. Because the scattered intensity is measured in arbitrary units that depend on unknown instru-

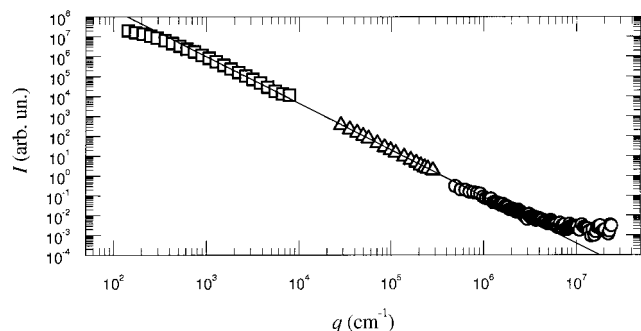


**Figure 2.** Scattered intensity for a 0.46% w/w solution of guar in D<sub>2</sub>O. The data were collected using USALS, SLS, and SANS instrumentation, and are scaled as described in the text. The line is a guide for the eye with a slope of  $-2.35$ .

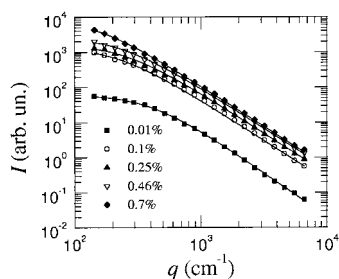


**Figure 3.** USALS data for guar in D<sub>2</sub>O, for several concentrations. The curves are labeled by the weight concentration. The lines are Fisher-Burford fits to the data.

mental factors, the relative intensities between data sets from each instrument are unknown. It was assumed that the data are continuous, and scaling factors were chosen on this basis to make the data lie on a single curve. The data span 5 decades in  $q$ , showing a roll-off to an incipient plateau at a very low scattering vector ( $q \approx 300 \text{ cm}^{-1}$ ), followed by a large power law region extending over almost 4 decades in  $q$ . A solid line with a power law exponent of  $-2.35$  is shown as a guide to the eye. A deviation from this power law behavior to a smaller slope at the highest measured scattering vectors (with a power law exponent of about 1) is also seen. This deviation represents local rigidity in the chain and is discussed elsewhere.<sup>16</sup>

Plateau formation at low scattering vectors normally indicates the crossover between the scattering from the internal structure of a molecule and that from uncorrelated, distinct molecules. As shown in Figure 2, however, plateau formation for guar in D<sub>2</sub>O occurs at a remarkably small scattering vector, corresponding to length scales on the order of  $100 \mu\text{m}$ , much larger than the size expected for a single chain. To quantify the size of these large structures, we tried Debye and Guinier fits, which gave poor agreement with the data. A fit of the data to a Fisher-Burford function,<sup>17</sup> on the contrary, was satisfactory (see Figure 3). The Fisher-Burford function has the form

$$I(q) = I(0)/[1 + (2/3)(qR_g)^2]^{d_f/2} \quad (3)$$

where  $R_g$  is the radius of gyration of the scatterer. This equation generalizes the Guinier form to fractal objects and is often used to describe the scattering from fractal aggregates. In fitting the data, we fixed the value of  $d_f$  to that obtained from the power law regime of the USALS data,  $d_f \sim 2.4$ , while  $I(0)$  and  $R_g$  were varied to obtain the best fit. For the guar solution shown in Figure 2, the fit yields  $R_g = 85 \mu\text{m}$ . Although there is some variation in the data reported in the literature,<sup>16</sup> the molecular weight of guar is estimated to be about 2 million,<sup>5</sup> corresponding to a size on the order of  $100 \text{ nm}$ , 3 orders of magnitude smaller

than  $R_g$ . Thus, USALS data indicate unambiguously the presence of large structures at a supramolecular scale. To obtain insight into the physical meaning of  $R_g$ , we show in Figure 3 USALS data for several guar concentrations  $c$ , ranging from 0.01% to 0.7% (w/w) in D<sub>2</sub>O together with the Fisher-Burford fits. The general trend is a shift in the position of the roll-off to lower scattering vectors as the concentration increases. This corresponds to an increase in the value of  $R_g$  obtained from the fit. We note that if  $R_g$  were the correlation length of an entangled polymer network, it would decrease with increasing concentration.<sup>18</sup> Therefore, despite the fact that the concentration is above the  $c^*$  expected for a single chain (as obtained from the intrinsic viscosity), the data indicate that  $R_g$  does not represent the correlation length of an entangled polymer network, but rather the size of supramolecular structures. It is then natural to consider these structures as aggregates consisting of more than one chain, whose size increases with  $c$ .

The existence of aggregates in guar solutions has been widely accepted;<sup>5</sup> however, their characterization has not been previously investigated. Light scattering is a valuable tool for determining their size and structure; however, it is essential to access the ultrasmall angles needed to probe these unusually large structures. The presence of aggregates is most likely due to the ability of guar molecules to form association complexes both inter- and intramolecularly. Recall that the galactose substitution along the mannose backbone is random, leading to regions of high and low substitution. It is believed that interactions mostly occur among galactose-poor regions of guar chain segments.<sup>8</sup> These interactions are noncovalent in nature and can have extended junction zones.<sup>19</sup> In fact, it is the very presence of the galactose units that makes the guar molecule soluble; these side units provide a steric barrier, preventing a more highly organized structure from forming.<sup>8,19</sup> The power law region at scattering vectors somewhat larger than those of the plateau suggests that the aggregates have fractal morphology, with a fractal dimension of 2.4. At larger scattering vectors, accessible by SLS, the scattering probes length scales on the order of  $100 \text{ nm}$ , the order of magnitude expected for single chains of guar molecules. Here, the fractal dimension is 2.3, higher than 2 and thus indicative of somewhat poor solvent conditions in D<sub>2</sub>O. For an ideal polymer, this suggests a slightly collapsed Gaussian, or random walk, conformation. While for unbranched polymers chain collapse is the only mechanism which would cause the fractal dimension to be higher than 2, for guar the increase of  $d_f$  may also be caused by "branching" due to intramolecular associations between regions which are galactose-poor. (Note that the small galactose side groups themselves do not contribute significantly to the fractal dimension on these length scales.) If branching through galactose-poor region association is occurring in guar, it is likely to increase with concentration, thus increasing the fractal dimension as well. Preliminary measurements indicate that this does indeed occur.

Speculations can be made as to the supramolecular organization of the system, although actual descriptions are difficult to confirm. The data suggest the presence of moderately polydisperse aggregates consisting of several guar chains. Some single chains and aggregates may exist freely in solution, while others are loosely connected. A few chains may belong to one or more aggregates. As the polymer concentration increases and inter- and intramolecular associations become even more prevalent, the size of these aggregate structures will likely increase, as indicated by USALS data. Moreover, the probability of having loosely connected multiaggregate structures also increases. The

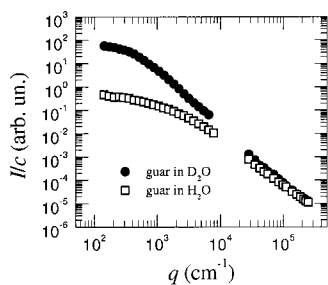


**Figure 4.** Normalized scattered intensity  $I/c$  for dilute solutions of guar in  $\text{H}_2\text{O}$  and  $\text{D}_2\text{O}$ . For all samples  $c = 0.038\%$  w/w, except for the USALS data for guar in  $\text{D}_2\text{O}$ , for which  $c = 0.01\%$  w/w.

result is a system which flows, yet contains chains and aggregates in both networked and free form. It should be noted that at higher guar concentrations ( $c \geq 1\%$  w/w) the system gels, indicating a highly interconnected network. Unfortunately, the persistence of bubbles in these solutions makes light-scattering measurements impossible since the scattering from bubbles overwhelms that from the guar, especially at very low angles. The mere presence of the aggregates indicates reduced solubility for guar. The large-scale fractal structures lead to a solution which is heterogeneous, affecting its viscoelastic behavior as well as the flow behavior. Such behavior is important industrially in thickening, extraction, and processing.

Figure 4 shows a comparison of the scattering from dilute solutions of guar in  $\text{H}_2\text{O}$  and  $\text{D}_2\text{O}$ , in the intermediate- and ultralow- $q$  vector range. All data were taken at  $c = 0.038\%$  w/w, except for the USALS curve for guar in  $\text{D}_2\text{O}$ , for which  $c = 0.01\%$  w/w. The data are normalized to the concentration for comparison purposes. (This normalization is justified by the fact that, at low  $c$ , the scattered intensity scales with concentration, as will be discussed below.) The curves exhibit some features in common as well as distinct differences. The common feature is the presence of a rollover at low  $q$ , which indicates, quite surprisingly, that aggregates are present even at very low concentrations, although they are smaller in size: about  $20\ \mu\text{m}$  in radius for a  $0.038\%$  solution in  $\text{H}_2\text{O}$  and about  $54\ \mu\text{m}$  in radius for a  $0.01\%$  solution in  $\text{D}_2\text{O}$ . We point out that the concentrations used in this comparison are a decade below the  $c^*$  that was calculated on the basis of intrinsic viscosity measurements (for  $\text{H}_2\text{O}$ ). Thus, guar solutions, even at rather low concentrations, do not exhibit classical polymer behavior, and caution must be taken in the use of  $c^*$  to describe the overlap concentration. The most remarkable differences are observed in the low- $q$  regime. The scattering from guar in  $\text{H}_2\text{O}$  is dramatically lower than that from the sample in  $\text{D}_2\text{O}$ , the difference being as large as a factor of 100. Moreover, the transition between the fractal regime and the plateau at very low  $q$  occurs at higher scattering vectors and is less sharp for the sample in  $\text{H}_2\text{O}$ . Both of these features suggest that aggregates are smaller when guar is dissolved in  $\text{H}_2\text{O}$ . The rollover is relatively gradual, indicating a broader distribution of sizes in  $\text{H}_2\text{O}$ , with small aggregates coexisting with larger structures. Collectively, these observations suggest a greater solubility of guar in  $\text{H}_2\text{O}$  than in  $\text{D}_2\text{O}$ . The SLS data confirm this picture. In fact, at intermediate scattering vectors, the fractal dimension in  $\text{H}_2\text{O}$  is lower than in  $\text{D}_2\text{O}$  (1.9 compared to 2.1, respectively). Although small, this difference is reproducible and is consistent with a greater solubility of guar in  $\text{H}_2\text{O}$ , since the increase of solubility in  $\text{H}_2\text{O}$  would lead to a less branched and less collapsed polymer conformation, consistent with the smaller fractal dimension measured. Further qualitative support for increased solubility of guar in  $\text{H}_2\text{O}$  is provided by the observa-

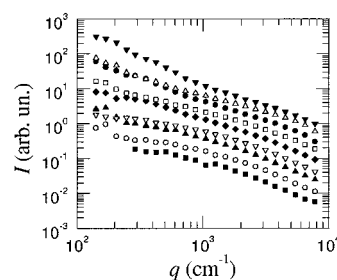


**Figure 5.** USALS data for guar in  $\text{H}_2\text{O}$ , for several concentrations. From top to bottom, concentration is 1.1%, 0.7%, 0.34%, 0.17%, 0.079%, 0.038%, 0.019%, 0.009%, 0.004% w/w.

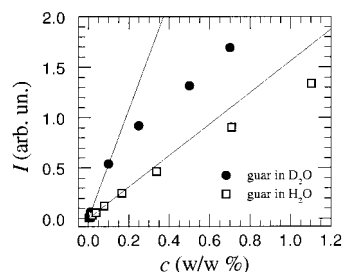


**Figure 6.** Concentration dependence of the scattered intensity for  $q = 6500\ \text{cm}^{-1}$ , for guar in  $\text{H}_2\text{O}$  and  $\text{D}_2\text{O}$ . The lines are linear fits through the origin to the data, for  $c \leq 0.1\%$ .

tion that, during sample preparation, it took considerably longer for the same amount of guar to dissolve in  $\text{D}_2\text{O}$  than in  $\text{H}_2\text{O}$ .

Ultra-low-angle scattering data from guar in  $\text{H}_2\text{O}$  at concentrations varying from 0.004% to 1.1% are plotted in Figure 5. The data are compared to structural features in  $\text{D}_2\text{O}$  systems as displayed in Figure 3. At concentrations of 0.038% and below, the data follow a trend similar to that seen for the  $\text{D}_2\text{O}$  solutions, although the roll-off is shifted to higher  $q$  and is less sharp, as discussed above. At higher concentrations, however, vestiges of plateau formation disappear as the data tend to increase more sharply at the lowest measured  $q$  values. This upward turn may represent the formation of even larger aggregate structures or, possibly, the beginning of microphase separation. Although such features are not present with the  $\text{D}_2\text{O}$  data, they may appear at even lower scattering vectors, out of the range of accessible  $q$ , reflecting the decreased solubility of guar in  $\text{D}_2\text{O}$ .

The differences between the behavior of guar in  $\text{H}_2\text{O}$  and  $\text{D}_2\text{O}$  are further exemplified by the concentration dependence of the scattered intensity in the low angle power law regime. Figure 6 shows this dependence for both  $\text{H}_2\text{O}$  and  $\text{D}_2\text{O}$  solutions at  $q = 6500\ \text{cm}^{-1}$ , the high- $q$  end of the USALS data sets. We assume that at this  $q$  value the power law regime is fully established. The lines in the graph are linear fits through the origin to the data at the lowest concentrations ( $c \leq 0.1\%$ ). Except at the lowest concentrations, the concentration dependence for the  $\text{D}_2\text{O}$  solutions is significantly sublinear. Since in the power law regime the scattered intensity is proportional to the total amount of material composing the fractal structures, this sublinear behavior suggests that the guar is more incompletely dissolved as its concentration increases; this confirms the reduced solubility of guar in  $\text{D}_2\text{O}$ . By contrast, deviations from the linear growth of  $I$  vs  $c$  are much less pronounced for guar in  $\text{H}_2\text{O}$ , reflecting the higher solubility.

The question naturally arises as to why there are such large differences in the solubility of guar in  $\text{H}_2\text{O}$  and  $\text{D}_2\text{O}$ . The properties of both solvents at  $25\ ^\circ\text{C}$  are listed in Table 1.<sup>20</sup> While both have similar dielectric constants and indices of refraction, the densities at  $25\ ^\circ\text{C}$  and the temperatures of maximum density are significantly different. The different values of the latter two

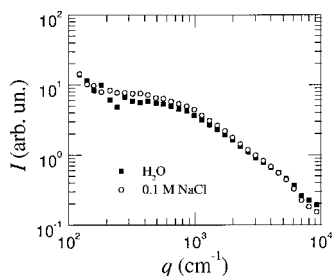


**Figure 7.** Comparison of the USALS intensity for cationic guar in H<sub>2</sub>O and in a 0.1 M aqueous solution of NaCl.

**TABLE 1**

|                  | dielectric constant | index of refraction | temp of max density (°C) |
|------------------|---------------------|---------------------|--------------------------|
| H <sub>2</sub> O | 78.304              | 1.3326              | 4                        |
| D <sub>2</sub> O | 77.937              | 1.3283              | 11.2                     |

parameters suggest dissimilarities in the molecular organization within the liquid state. These differences were found to be critical when the decreased solubility of lysozyme in D<sub>2</sub>O as compared to H<sub>2</sub>O was explained.<sup>21</sup> In fact, solubility vs temperature curves in both solvents were found to be shifted by 7.2 °C, the same as the difference in the temperatures of maximum density. It is known that the solubility of a molecule often depends on the orientation and structure of the solvent molecules immediately surrounding it,<sup>22</sup> and it seems reasonable that H<sub>2</sub>O and D<sub>2</sub>O molecules may orient differently around the guar molecule, thus affecting solubility in different manners.

To stress the central role played by inter- and intramolecular associations in guar solutions, we also present USALS data on cationic guar, in both unscreened (pure H<sub>2</sub>O) and screened (0.1 M NaCl in H<sub>2</sub>O) conditions. In the unscreened case, the guar is fully charged and repulsion between and within chains should be maximized. Typically, unconnected polyelectrolytes in a fully charged state are fully extended in good solvent conditions, with intermediate- $q$  range power law behavior close to 1.<sup>18</sup> In 0.1 M NaCl, the Debye screening length is about 10 Å; reduced inter- and intrachain repulsions are to be expected at length scales larger than the screening length. However, the data presented in Figure 7 for 0.46% w/w cationic guar solutions show virtually no differences in the low- $q$  regime for screened and unscreened solutions. Aggregates are present in both solutions, even when electrostatics charges are not screened, and they are the same size. Therefore, aggregates appear to be an inherent part of guar solutions, charged or uncharged, and for both H<sub>2</sub>O and D<sub>2</sub>O. Their presence dominates the scattering profile, preventing structure on all other length scales (other than at the persistence length at high  $q$ ) from being detected. The plateau at ultralow  $q$  is the only measurable length scale for D<sub>2</sub>O and H<sub>2</sub>O systems, assuming that other features are not hidden within the gaps between data sets from different instruments (see Figures 2 and 4). This makes the determination of the size of a single chain, and hence of the molecular weight, impossible. This finding is important because Zimm plot measurements on these systems often appear to be reasonable, although they give molecular weight estimations widely varying from 0.5 to several million.<sup>5,16</sup> However, when the data are plotted on a double logarithmic  $I$  vs  $q$  scale, no plateau (or Guinier) region exists, as is necessary to correctly determine the size. In addition to variations in the guar molecule from different sources and processing procedures, the method chosen for data analysis may therefore be another reason why molecular weight determinations differ significantly among studies reported.

## Conclusions

The conformation and supramolecular organization of guar solutions in H<sub>2</sub>O and D<sub>2</sub>O as determined from scattering techniques are presented. The scattering profiles indicate plateau formation at ultralow scattering vectors and a large power law region spanning several decades in  $q$ . The plateau region is believed to result from aggregates that have fractal morphology, and whose radius is on the order of 10–100  $\mu$ m, depending on the concentration and the solvent. At larger scattering vectors a fractal dimension close to 2 is found, indicating near  $\Theta$  solvent conditions and suggesting the possibility of fractally arranged “branches”, or inter- and intramolecular associations thought to stem from regions that are galactose-poor. Aggregates were found for both neutral and cationic guar solutions, with the latter tested in both electrostatically screened and unscreened conditions. The presence of the aggregates dominates the scattering profile, making structures at other length scales undetectable with light scattering. Consequently, structure on the length scale on the order of the size of single guar chains is not seen, making determinations of the molecular weight via Zimm plots unreliable.

Significant differences in the solubility of neutral guar in both solvents were found, all consistent with greater solubility in H<sub>2</sub>O. Smaller aggregates were confirmed by a decrease in the scattering intensity at the lowest measured  $q$  values by 2 orders of magnitude and by a shift in plateau formation to higher scattering vectors. The transition between plateau and power law behavior spans a larger scattering vector range in H<sub>2</sub>O, suggesting a broader distribution of aggregate sizes. The intermediate power law regime shows a small decrease in the fractal dimension from 2.2 (in D<sub>2</sub>O) to 1.9 (in H<sub>2</sub>O), consistent with increased solubility in H<sub>2</sub>O. Finally, the low- $q$  dependence of the scattering intensity on concentration is almost linear for H<sub>2</sub>O systems, while remarkably sublinear for D<sub>2</sub>O systems, consistent with reduced solubility of guar in D<sub>2</sub>O. These differences are surprising, considering how closely related both solvents are; they may stem from a difference in the molecular organization of the solvent molecules surrounding the polymer chain. This solvent sensitivity suggests that extrapolation of structural features from high- $q$  data obtained from neutron scattering must be done with care.

The data presented in this work indicate that aggregates are prominent in guar systems and may have important contributions to the viscoelastic behavior of the solution, depending on how they are interconnected. This work also hints of possibly greater differences in structure, and hence viscoelastic behavior, when other solvent conditions are present. Indeed, we found that the structural and viscoelastic properties of aqueous guar solutions can be dramatically varied by adding isopropyl alcohol. These experiments will be reported in a forthcoming paper.<sup>23</sup>

**Acknowledgment.** Jyotsana Lal from IPNS, Argonne National Laboratories, is gratefully acknowledged for her assistance with collecting neutron scattering data, data analysis, and many valuable discussions. We thank Animesh Goswami and Olivier Anthony for purifying the guar and Anthony Homack, Denis Wozniak, and Ed Lang for their help with sample preparation and instrument operation for small-angle neutron scattering. We also thank Jeanne Chang and Christian Robelin for the intrinsic viscosity measurements. Last, we are grateful to Robert Prud'homme and Frederic Simonet for many valuable discussions. We thank Paul Joel Dérian and Jean Gauthier-Lafaye for providing financial support within Rhodia Inc. The work at the

University of Pennsylvania was supported by NASA (Grant NAG3-2058) and NSF (Grants DMR-9631279 and DMR-9704300). Also, this work has benefited from the use of the Intense Pulse Neutron Source at Argonne National Laboratory. This facility is funded by the U.S. Department of Energy, BES-Materials Science, under Contract W-31-109-Eng-38.

### References and Notes

- (1) (a) Rhodia Inc. (b) University of Pennsylvania. (c) Present address: GDPC cc 26, Université Montpellier II, P. E. Bataillon, Montpellier 34000, France. E-mail: lucacip@gdpc.univ-montp2.fr. (d) Present address: Institut de Physique, Université de Fribourg, CH-1700 Fribourg, Switzerland. (e) Present address: Department of Physics and DEAS, Harvard University, Cambridge, MA 02138.
- (2) Fox, J. E. In *Thickening and Gelling Agents for Food*, 2nd ed; Imeson, A., Ed.; Blackie Academic Professional: New York, 1997; pp 262–283.
- (3) Prud'homme, R. K.; Constien, V.; Knoll, S. *Adv. Chem. Ser.* **1989**, 223, 89.
- (4) Pugliese, P.; Himes, G.; Wielinga, W. *Cosmetics Toiletries* **1990**, 105, 105.
- (5) Brode, G. L.; Goddard, E. D.; Harris, W. C.; Salensky, G. A. In *Cosmetic and Pharmaceutical Applications of Polymers*; Gebelein, C. G., Cheng, T. C., Yang, V. C., Eds.; Plenum: New York, 1991; pp 117–128.
- (6) Robinson, G.; Ross-Murphy, S. B.; Morris, E. R. *Carbohydr. Res.* **1982**, 107, 17.
- (7) Patel, S. P.; Patel, R. G.; Patel, V. S. *Int. J. Biol. Macromol.* **1987**, 9, 314.
- (8) Whitcomb, P. J.; Gutowski, J.; Howland, W. W. *J. Appl. Polym. Sci.* **1980**, 25, 2815.
- (9) Doublier, J. L.; Launay, B. *J. Texture Stud.* **1981**, 12, 151.
- (10) Morris, E. R. *Br. Polym. J.* **1986**, 18, 14.
- (11) Molyneux, P. In *Water-Soluble Polymers: Synthesis, Solution Properties, and Applications*; Shalaby, S. W., McCormick, C. L., Butler, G. B., Eds.; ACS Symposium Series; American Chemical Society: Washington, DC, 1991; Vol. 467, p 232.
- (12) Teixeira, J. In *On Growth and Form: Fractal and Non-Fractal Patterns in Physics*; Stanley, H. E., Ostrowsky, N., Eds.; Nijhoff: Boston, 1986; pp 154–155.
- (13) Rubinstein, M.; Colby, R. H. *Phys. Rev. Lett.* **1994**, 73, 2776.
- (14) Cipelletti, L.; Weitz, D. A. *Rev. Sci. Instrum.* **1999**, 70, 3214.
- (15) Gittings, M. R.; Lal, J.; Dérian, P. J.; Marques, C. In *Polysaccharide Applications: Cosmetics and Pharmaceuticals*; El-Nokaly, M. A., Soini, H. A., Eds.; ACS Symposium Series; American Chemical Society: Washington, DC, 1999; Vol. 737, p 287.
- (16) Vijayendran, B. R.; Bone, T. *Carbohydr. Polym.* **1983**, 4, 299.
- (17) Fisher, M. E.; Burford, R. J. *Phys. Rev. A* **1967**, 156, 583.
- (18) de Gennes, P. G. *Scaling Concepts in Polymer Physics*; Cornell University Press: London, 1979.
- (19) Rees, D. A. *Polysaccharide Shapes*; Chapman & Hill: London, 1977.
- (20) Weast, R. C., Ed. *Handbook of Chemistry and Physics*, 57th ed.; CRC Press: Cleveland, 1976.
- (21) Gripon, C.; Legrand, L.; Rosenman, I.; Vidal, O.; Robert, M. C.; Boué, F. *J. Cryst. Growth* **1997**, 178, 575.
- (22) Paulitis, M. E. *Curr. Opin. Colloid Interface Sci.* **1997**, 2, 315.
- (23) Gittings, M. R.; Cipelletti, L.; Trappe, V.; Weitz, D. A.; Lal, J.; Marques, C. Manuscript in preparation.